Article

Direct genome-scale screening of *Gluconobacter oxydans* B58 for rare earth element bioleaching

Check for updates

Sabrina Marecos [1], Brooke Pian[1,4], Sean A. Medin[1,4], Alexa Schmitz[1,4], Melinna Andrade [1], Mingming Wu [1], J. Brian Balta[2], Esteban Gazel [2], Megan Holycross[2], Matthew C. Reid[3] & Buz Barstow [1] ✉

The transition to a sustainable energy economy will require an enormous increase in the supply of rare earth elements (REEs). Bioleaching offers a promising alternative to conventional hydrometallurgical methods for REE extraction from low-grade ores. However, exploiting this potential remains challenging due to large gaps in our understanding of the genetics involved, and inadequate biological tools to address them. We generated a highly non-redundant whole-genome knockout collection for the bioleaching microbe *Gluconobacter oxydans* B58, reducing redundancy by 85% compared to the previous best collection. This new collection was directly screened for bioleaching neodymium from a synthetic monazite powder, identifying 89 genes important for bioleaching, 68 of which have not previously been associated with this mechanism. We conducted bench-scale experiments to validate the extraction efficiency of promising strains: 8 demonstrated significant increases in extraction by up to 111% (δGO_1598, disruption of the gene encoding the orotate phosphoribosyltransferase enzyme PyrE), and one strain significantly reduced it by 97% (δGO_1096, disruption of the gene encoding the GTP-binding protein TypA). Notable changes in pH were only observed for 3 strains, suggesting an important role for non-acid mechanisms in bioleaching. These findings provide valuable insights into further enhancing REE-bioleaching by *G. oxydans* through genetic engineering.

Rare Earth Elements (REEs; including the lanthanides ($Z = 57$ to 71), scandium, and yttrium) are crucial ingredients in present-day sustainable energy technologies including wind turbines[1,2] and electric vehicles[3], and in future ones like high-temperature superconductors[4–7]. As a result of this, the demand for REEs is expected to grow by between 3- and 7-fold by 2040[8]. However, existing hydrometallurgical methods for REE mining pose considerable environmental risks[9–11].

The growing demand for an environmentally-friendly supply chain for REEs has fueled interest in biotechnological processes for REE mining and recycling[9,12–20]. Bioleaching solubilizes metals from minerals and end-of-life feedstocks with a microbially-secreted mineral-dissolving cocktail called a biolixiviant[13,14,16,21–23]. In recent years, the search for more efficient bioleaching strategies has gained significant interest[23–25].

The Generally Regarded As Safe (GRAS) acidophilic bacterium *Gluconobacter oxydans*[26–29] has played a significant role in bioleaching research over the past decade[14,21,30–33]. This microbe offers a unique capability for secretion of organic acids[21,29,34] and creation of a highly acidic biolixiviant (primarily containing gluconic acid[14]) which is particularly effective for recovering REEs from sources including minerals like allanite[15]; industrial residues like phosphogypsum[30]; red mud[35], and blast furnace slag[36]; and recycled materials like fluid cracking catalyst (FCC)[21], nickel-metal-hydride (NiMH) batteries[37], and retorted phosphor powder (RPP)[16,21,35].

We have already improved bioleaching of REEs by *G. oxydans* by first identifying genes involved in acid production with high-throughput screening[16], and then engineering their regulation[15]. We increased REE-bioleaching from the REE-containing mineral allanite by up to 73% by up-regulating the membrane-bound glucose dehydrogenase, *mgdh*, and knocking out the phosphate signaling and transport system *pstS*[15].

Despite progress in enhancing REE-bioleaching with *G. oxydans*, further genetic improvements may be necessary to allow it to leapfrog traditional thermochemical extraction processes[33,38]. One way to further improve it is to target the regulation of additional genes implicated in

[1]Department of Biological and Environmental Engineering, Cornell University, Ithaca, NY, USA. [2]Department of Earth and Atmospheric Sciences, Cornell University, Ithaca, NY, USA. [3]School of Civil and Environmental Engineering, Cornell University, Ithaca, NY, USA. [4]Present address: REEgen Inc., Praxis Center for Venture Development, Cornell University, Ithaca, NY, USA. ✉e-mail: bmb35@cornell.edu

bioleaching by acid production screens[16]. However, it is proposed that metal solubilization in bioleaching happens through three processes: acidolysis via acid production, complexolysis by creating complexes between metal ions and organic compounds, and redoxolysis, which involves electron transfer and oxidative reactions[33]. *G. oxydans'* biolixiviant appears to be more effective than pure gluconic acid controls at the same pH[21]. This could suggest that the biolixiviant contains additional components that amplify its effectiveness[21,22,30,32,39].

We hypothesize that further characterizing the mechanism of bioleaching and then engineering the composition of the biolixiviant is the route to future significant increases in bioleaching efficiency. But the acid production screens that we have used to date may not be sensitive to complexolysis and redoxolysis. Thus, to fully characterize the biolixiviant, it is necessary to identify genes directly linked to bioleaching, rather than just acid production alone. In this study, we conducted a genome-scale screen of a new quality-controlled *G. oxydans* B58 whole genome knockout collection with a high-throughput assay designed to directly identify genes involved in REE-bioleaching.

Results

G. oxydans' quality-controlled collection is 85% smaller than previous collection

To facilitate direct high-throughput screening of mineral-dissolution, we built a highly non-redundant Quality-Controlled (QC) whole genome knockout collection for *G. oxydans* B58. The QC collection was built by removing redundancy from our earlier condensed collection (CC) of *G. oxydans* transposon disruption mutants[16]. Throughout this article, we refer to transposon disruption mutants with a "δ" symbol (as opposed to a "Δ" symbol for clean deletion mutants; e.g., δ*GO_1096*).

In total, the QC collection contains a single carefully chosen transposon disruption mutant for 2733 non-essential genes in the *G. oxydans* B58 genome arrayed onto 57 checker-boarded 96-well plates (Supplementary Data 1). The QC collection is 94% smaller than our *G. oxydans* saturating-coverage transposon mutant collection used to source all mutants in our earlier work (containing 49,256 mutants)[16], and 85% smaller than our previous best curated collection (17,706 mutants)[16]. An overview of QC collection construction is shown in Fig. 1, and collection statistics are shown in Table 1. Full details of QC collection construction can be found in "Materials and Methods".

### Genome-scale screen of QC collection identifies 68 genes not previously implicated in REE-bioleaching

We performed a genome-scale screen of the QC collection to identify gene disruption mutants with differential REE-bioleaching capabilities. We developed a rapid microplate-based colorimetric assay with the REE-chelating dye Arsenazo-III (As-III) to screen for REE extraction[18,40,41] from a synthetic monazite powder (Fig. 2A, B) (monazite is the mineral host for REEs at the Mountain Pass Mine in California, one of the largest REE mines in the world[10]). Unlike natural monazite (which contains multiple light lanthanides), this synthetic mineral contains just neodymium (Nd)[42], allowing greater consistency in the determination of extraction efficiency. Two synthetic monazite powder batches were synthesized (Mon1 and Mon2) as described by Balta et al.[42], presenting minor differences in Nd-phosphate composition (Supplementary Data 2). Mon1 was composed of monazite-Nd ($NdPO_4$), rhabdophane-Nd ($NdPO_4 \cdot 2H_2O$), and neodymium oxyphosphate (Nd_3PO_7). In contrast, Mon2 consisted solely of monazite-Nd and rhabdophane-Nd.

Mon1 demonstrated greater dissolution than Mon2 during bioleaching. This discrepancy is likely due to the elevated concentration of neodymium oxides in Mon1 (Supplementary Data 2), along with the higher thermal expansion and oxidation state of the Nd_3PO_7[43,44]. We utilized both Mon1 and Mon2 in our screening to leverage their distinct characteristics. Mon1 enhanced the detection sensitivity for potential hits in the initial preliminary survey, thereby expanding the selection pool for subsequent validation. Mon2, being less reactive, allowed for the isolation of the most significant outliers in the initial survey, offering a closer analog to bioleaching with natural monazite.

Our preliminary survey (Supplementary Data 3A) identified 89 gene disruptions that produced significant changes in Nd extraction from the Mon1 synthetic monazite (Fig. 2C). These hits included disruptions of 21 genes previously linked to acidification[16] and 68 genes that have not previously been linked to bioleaching (Supplementary Data 3B).

A follow-up screen of these 89 mutants found 6 mutants that produced statistically significant changes to Nd-extraction from the Mon2 synthetic monazite (Supplementary Data 3C, Table 2). We included 6 additional mutants for further analysis based on their prominence in the initial Mon1 Nd-extraction survey (Table 2).

A. Quality-Controlled Collection Construction
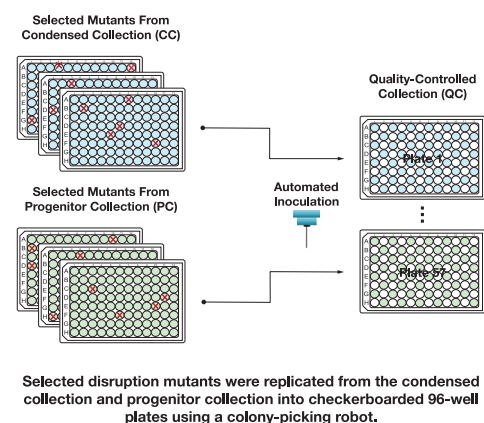
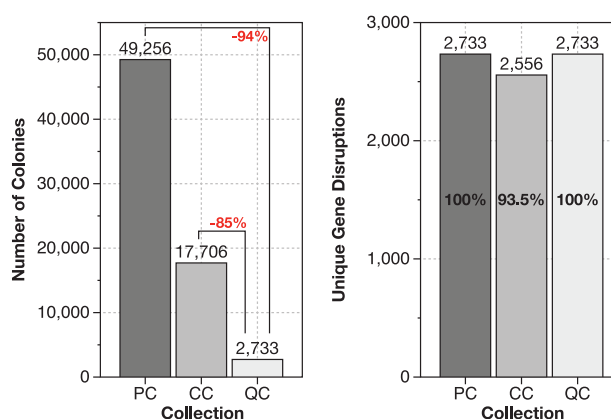### B. *G. oxydans* Quality-Controlled Collection Statistics

Fig. 1 | Construction of a quality-controlled (QC) collection containing a single disruption mutant for 2733 genes in *G. oxydans'* genome. A The QC collection was built by choosing the best available mutants from an earlier condensed collection (CC) of *G. oxydans* mutants[16], and by supplementation from the originating saturating-coverage transposon collection (Progenitor Collection or PC)[16]. Mutants were transferred from the earlier collections by fluid transfer into fresh 96-well plates with a colony picking robot. **B** The QC collection contains 2733 unique mutants distributed across 57 checker-boarded 96-well plates. This collection represents a 94% reduction in size from the PC, and an 85% reduction in size from the CC, indicated in red. It is worth noting, that the CC collection contained disruption mutants with confirmed identity for 2556 genes (93.5% of the 2733 genes disrupted in the PC), whereas the QC collection aims to include a disruption mutant for 100% of genes disrupted in the PC.

Table 1 | Overview of *G. oxydans* B58 quality-controlled (QC) whole genome knockout collection statistics

Collection of Origin	Number of Mutants	Distance from Translation Start				
		< 50 bp	≥ 50 bp	≤ 0.5	> 0.5	≥ 50 bp AND ≤ 0.5
Progenitor Collection (PC)	285	21	264	172	113	153
Condensed Collection (CC)	2448	240	2208	2037	411	1797
Total (QC Collection)	2733	261	2472	2209	524	1950

This table summarizes the transposon location characteristics of the mutants derived from the progenitor collection (PC) and condensed collection (CC) used to generate the QC collection. Mutants were categorized based on the distance of the disruption from the translation start of the gene: less than 50 base pairs, at least 50 base pairs, within 0.5 fractional distance of the gene, beyond 0.5 fractional distance, and disruptions located at least 50 base pairs downstream and within 0.5 fractional distance, which were considered the optimal locations for disruption of gene function.
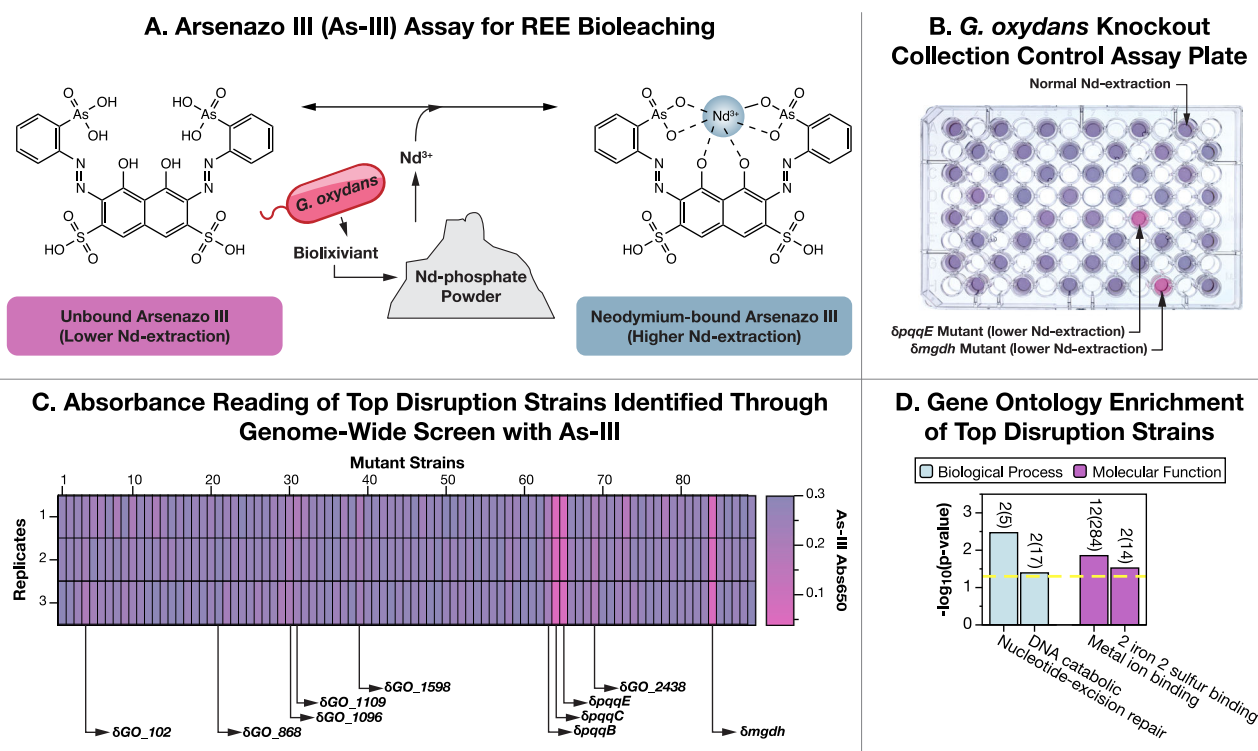

Fig. 2 | Direct bioleaching screening of the quality-controlled whole genome knockout collection of *Gluconobacter oxydans* identifies 68 gene disruptions not previously associated with bioleaching. A We developed a rapid 96-well plate based high-throughput screen for REE-bioleaching that uses a colorimetric assay with the Arsenazo III (As-III) REE-chelating dye in presence of synthetic monazite. This assay directly detects REE release, facilitating the identification of disruptions with differential bioleaching capabilities. **B** Color differences in each well identify which genes control bioleaching. Gene disruptions that reduce bioleaching leave the As-III dye unbound and pink, while disruptions that increase bioleaching turn the dye blue.

C The genome-scale screening of the QC collection identified 89 hits including 68 gene disruptions not previously associated with the bioleaching capabilities of *G. oxydans*. **D** Gene Ontology (GO) Enrichment was performed with a Fisher's Exact Test ($p < 0.05$, yellow dashed line) to analyze the hits identified. Significantly enriched GO terms with at least 2 representatives are displayed, and numbers above the bars represent the significant hits out of the total annotated genes associated with that gene ontology in the genome of *G. oxydans* (the full list of GO terms can be found in Supplementary Data 3D). Only terms belonging to the Biological Process and Metabolic Function GO groups were significantly enriched.

Metal binding and DNA repair gene ontologies are highly enriched among bioleaching hits

The 68 genes not previously associated with REE-bioleaching that were identified through the initial Mon1 REE-extraction survey were analyzed for gene ontology (GO) enrichment with topGO[45]. A total of four GO terms were found to be significantly enriched ($p < 0.05$ by Fisher's Exact Test) and to be associated with more than one gene (Supplementary Data 3D). These four enriched GO terms belong to the biological process (BP) and molecular function (MF) groups. No significant terms belonging to the cellular component group were found.

The two most statistically significantly enriched GO terms are metal ion binding and nucleotide-excision repair (Fig. 2D, Supplementary Data 3D). We speculate that the disruption of these genes affects bioleaching indirectly by modifying the expression of metabolic pathways that produce metal-solubilizing compounds. For example, metal ion binding proteins are often associated with signaling, sensing, and regulation[46–49], suggesting that their disruption could alter *G. oxydans*' bioleaching capabilities. Similarly, disruption of the nucleotide-repair system could impair the ability of *G. oxydans* to respond to damage generated by oxidative stress resulting from initial biolixiviant production[50,51] and thus alter further biolixiviant production.

Gene disruptions of interest demonstrate significant changes in bioleaching

The 12 gene disruption mutants that were highlighted by the Mon1 and Mon2 high-throughput assays (Table 2) were validated through bench-scale experiments where bioleaching was measured by Inductively Coupled Plasma—Mass Spectrometry (ICP-MS) (Fig. 3, Supplementary Data 4A). When compared to the proxy wild-type strain (pWT) (See "Materials and Methods"), 9 of the 12 disruption mutants generated
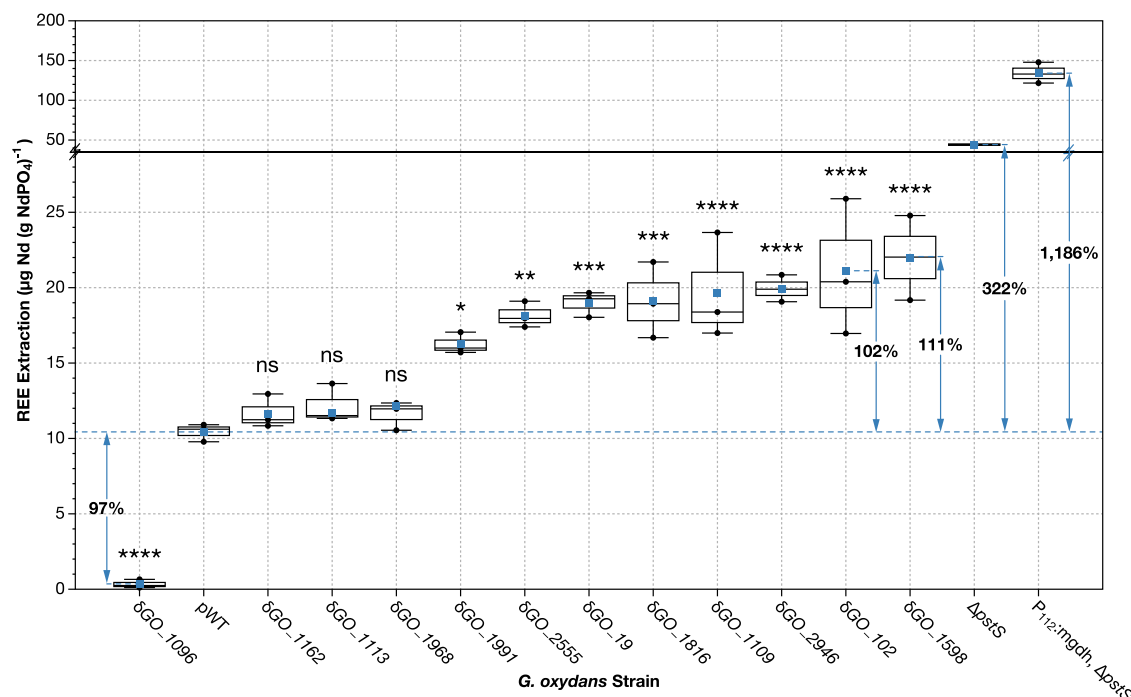
Fig. 3 | Identified *G. oxydans* gene disruptions raised REE-bioleaching by up to 111% or lowered it by 97%. Direct measurement of bioleaching extraction was performed on disruption mutants of interest following bioleaching experiments with synthetic monazite, using ICP-MS analysis. REE extractions were analyzed with pairwise comparisons among disruption mutants ($n = 3$) and pWT ($n = 3$). Levels of extraction significantly different from pWT are labeled with asterisks (*$p < 0.05$; **$p < 0.01$; ***$p < 0.001$, ****$p < 0.0001$) or "ns" if $p > 0.05$, denoting statistical significance after Bonferroni-corrected t-tests ($N = 12$). Blue squares indicate the mean extraction for each mutant, the center line denotes the median, boxes show the upper and lower quartiles, and whiskers extend to the range of data points within 1.5 times the interquartile range. Strains δGO_1162, δGO_1113, and δGO_1968 did not show statistically significant changes in extraction compared to pWT. Only one disruption mutant, δGO_1096, decreased bioleaching, demonstrating a 97% reduction in extraction. Current best-performing engineered strains, *G. oxydans* Δ$pstS$ (single knockout) and *G. oxydans* P$_{112}$:$mgdh$, Δ$pstS$ (up-regulation and knockout), were included to contrast the extractions of the tested disruption mutants. Significant changes in extraction efficiency compared against the WT strain can be found in Supplementary Fig. 1.

significant changes in bioleaching ($p < 0.05$). Eight disruption mutants produced greater (with increases of between 56 and 111%) Nd-bioleaching than pWT, while only one mutant (δGO_1096) produced a reduction (−97%) in bioleaching (Fig. 3). When compared to the wild-type strain (WT), all 12 disruption mutants tested produced significantly different extractions ($p < 0.01$) (Supplementary Fig. 1), showing increases from 75 to 231%, and a 95% reduction by δGO_1096. The changes in extraction efficiency relative to WT after cell density normalization (Table S1) closely align with the results presented in Fig. 3. This complementary data supports our findings and validates our use of pWT as a reference strain.

Although the increases in Nd-bioleaching achieved by 9 of the newly identified gene disruptions are substantial, they are notably smaller than those produced by our current two best-performing strains—*G. oxydans* Δ$pstS$ and *G. oxydans* P$_{112}$:$mgdh$, Δ$pstS$[15]—which demonstrated 322% and 1186% increases over pWT (Fig. 3), and 564% and 1922% over WT, respectively (Supplementary Fig. 1).

Overexpression of gene *GO_1096* increases bioleaching
We successfully engineered a markerless deletion strain, ΔGO_1096, and an overexpression strain, P$_{112}$:GO_1096 (Supplementary Fig. 2), for further assessment of *GO_1096*'s effects on bioleaching performance. The overexpression strain, P$_{112}$:GO_1096, demonstrated a significant increase in extraction efficiency compared to WT, with a 64% improvement (Fig. 5, Supplementary Data 4B), underscoring the positive regulatory role of *GO_1096* in bioleaching. We performed relative gene expression analysis of P$_{112}$:GO_1096, which revealed a 7.6-fold increase in *GO_1096* expression (Supplementary Fig. 2B, C); however, this substantial upregulation did not directly translate into a proportional increase in extraction efficiency. Interestingly, while the disruption of *GO_1096* led to a pronounced

reduction in bioleaching (Fig. 3), ΔGO_1096 did not exhibit the same effects on extraction efficiency (Fig. 5).

Many gene disruptions of interest do not affect biolixiviant pH
The pH of the biolixiviants produced by the 12 gene disruption mutants selected were measured (Fig. 4). Unsurprisingly, given our focus on identifying mutants absent in an acid-production screen, yet still noteworthy, 9 of the 12 mutants did not exhibit significant changes to biolixiviant pH when compared to a proxy wild-type strain of *G. oxydans*. Only the δGO_102, δGO_1096, and δGO_1109 mutants produced statistically significant changes to biolixiviant pH (Fig. 4). δGO_102 and δGO_1109 produced very modest reductions in biolixiviant pH of 0.06 and 0.07 units respectively, which are only barely above the precision-threshold of a pH meter. δGO_1096 produced a large increase in biolixiviant pH of 0.55 units.

Discussion
The generation of the QC collection facilitates the implementation of cost-effective and elaborate screening methods[52,53]. The curated collection encompasses disruption mutants for 2733 genes, one single representative for almost every non-essential gene in *G. oxydans*' genome[16]. The reduction in redundancy is crucial to improve the utility of a knockout collection, improving its value as a practical tool for the exploration of gene function[53,54]. This streamlined collection was essential for conducting a technically challenging genome-scale screen for REE-bioleaching, leading to the identification of previously uncharacterized aspects of this mechanism. To our knowledge, this study represents the first direct whole genome screening for bioleaching of any mined metal.

In total, we identified 89 gene disruptions involved in Nd-bioleaching from synthetic monazite. Notably, 21 genes implicated in acidification, previously reported[16], were among the hits found through this screen,

corroborating their direct involvement in REE-bioleaching. This outcome verifies the reliability of our As-III screen for Nd-bioleaching but also underscores some challenges related to reduced sensitivity. However, we also identified an additional 68 gene disruptions that were tested in our earlier assays but were not implicated in bioleaching. Out of 12 disruption mutants selected for further analysis, 9 did not produce any statistically significant change in pH (Fig. 4). This indicates that the new screen is more comprehensive than pH indicator screens for acid production. Furthermore, these results suggest that additional components might be present during bioleaching by *G. oxydans*[13,30], potentially increasing solubilization.

Notable and significant changes in bioleaching were validated by ICP-MS through bench-scale experiments (Figs. 3 and 4). Out of the 12 mutants selected for verification, only one (δGO_1096) reduced extraction, suggesting that this gene normally facilitates bioleaching. In contrast, 11 of the mutants appear to regulate bioleaching, and their disruption removes the inhibitory controls on it.

Three results (δGO_1096, δGO_1991, and δGO_1968) imply that changes in stress response pathways can both improve or impair the bioleaching mechanism. This notion has been discussed by Sousa et al. after

observing increased resistance to acetic acid at specific levels of oxidative stress in *Saccharomyces cerevisiae*[55].

Disruption of the gene encoding Formamidopyrimidine-DNA Glycosylase Fpg (GO_1968; belonging to both the metal ion binding and nucleotide excision repair gene ontologies terms) increased bioleaching. Fpg is a glycosylase involved in the repair of DNA damage caused by oxidative stress[56], and its disruption might lead to a heightened cellular response. For instance, it has been shown that certain levels of mistranslation can improve *Escherichia coli*'s tolerance to oxidative stress[51]. The metabolic response to accumulated DNA damage could involve transcription errors and shifts in secondary metabolite production. Such shifts might influence the types or quantities of solubilizing compounds produced by *G. oxydans*. Moreover, the gene coding for the Efflux ABC Transporter for Glutathione CycD (GO_1991) plays a role in redox balance within the periplasm during oxidative stress conditions[57], and its disruption also increases bioleaching.

Notably, only a single gene disruption led to a decrease in bioleaching efficiency (δGO_1096). GO_1096 codes for the GTP-binding protein TypA which has been linked to stress response[58]. This suggests that its disruption might hamper *G. oxydans*' ability to adapt to the stress generated during bioleaching, thereby diminishing efficiency. δGO_1096 was the only mutant that increased biolixiviant pH (out of only 3 that changed the pH at all). This result suggests TypA may facilitate acid-mediated bioleaching as well as non-acid bioleaching. We suspect that this gene was not found in our earlier acid-production screen[16] because we swapped the GO_1096 disruption mutant used in our original curated collection[16] for a new choice that was more likely to disrupt gene function. Interestingly, δGO_1096's increase in biolixiviant pH is modest compared to those produced by mutants identified in our previous screen that produced similar reductions in REE-extraction. For example, disruption of the *tldD* gene, necessary for the synthesis of the PQQ molecule (a cofactor for the membrane-bound glucose dehydrogenase), produced a 92% reduction in REE-extraction (admittedly from a different substrate) but raised biolixiviant pH by ≈ 0.7 units[16].

Furthermore, we observed that the disruption of three genes involved in gene expression increased bioleaching: GO_1162 encoding the phosphate regulon regulatory protein PhoB, GO_1109 encoding a LysR substrate binding domain, and GO_1816 encoding the transcriptional regulator YafY.

PhoB is involved in the regulation of inorganic phosphate (Pi) homeostasis[59]; it can positively or negatively regulate phosphate uptake in the presence of excess or limited Pi[60]. The disruption of GO_1162 only showed significant changes in bioleaching when compared to the wild-type strain (Fig. 3, Supplementary Fig. 1), indicating that this effect may not be fully caused by a loss of function. However, it is possible that disrupting this transcriptional activator can cause cells to lose the ability to modulate the phosphate regulon[61], potentially leading to continuous phosphate-scavenging. Such dysregulation could explain the slight increase
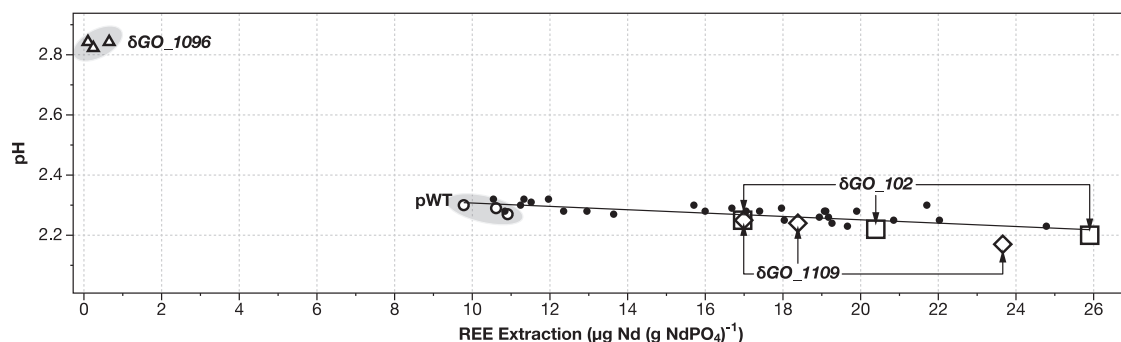
Table 2 | Selected gene disruptions for direct measurement of bioleaching

Gene Identifier	Feature Disrupted	Extraction Against pWT (%)
GO_1096	GTP-binding protein TypA/BipA	−97
GO_1598	Orotate phosphoribosyltransferase (EC 2.4.2.10)	+111
GO_102	hypothetical protein	+102
GO_1109	Transcriptional regulator, LysR family	+89
GO_1113	Xanthine and CO dehydrogenases maturation factor, XdhC/CoxF family	+12
GO_2555	hypothetical protein	+74
GO_2946	hypothetical protein	+91
GO_1162	Phosphate regulon transcriptional regulatory protein PhoB (SphR)	+11
GO_19	TonB-dependent receptor	+82
GO_1968	Formamidopyrimidine-DNA glycosylase (EC 3.2.2.23)	+17
GO_1991	Efflux ABC transporter for glutathione/L-cysteine, CydC subunit	+56
GO_1816	Transcriptional regulator, YafY family	+83

This table lists the selected gene disruption mutants for analysis, specifying their gene identifiers and disrupted features. It also presents the percentage change in extraction efficiency compared to pWT, where positive values indicate enhanced bioleaching and negative values denote a reduction.

Fig. 4 | Only three of the identified *G. oxydans* gene disruptions produce statistically significant changes in biolixiviant pH. REE extraction and biolixiviant pH were plotted for each strain selected for direct bioleaching measurement. Strain replicates that significantly changed the biolixiviant pH compared to proxy wild-type are indicated as follows, pWT "○", δGO_102 "□", δGO_1109 "◊", and δGO_1096 "△". Other gene disruptions with data points falling within the model are represented as "•", including data points for δGO_19, δGO_1113, δGO_1162, δGO_1598, δGO_1816, δGO_1968, δGO_1991, δGO_2555, and δGO_2946.
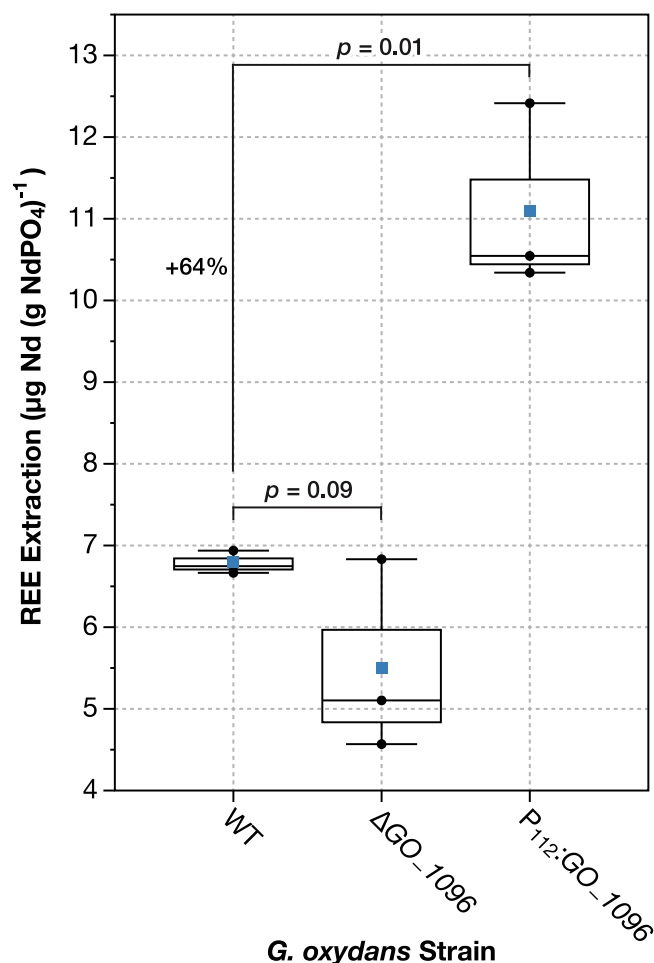
Fig. 5 | Genome-scale screening successfully identifies genetic engineering target to improve bioleaching. Mutant strains consisting of a clean deletion and an overexpression of the gene *GO_1096* were generated to test a selected hit as a target for genetic engineering. Extraction efficiency was determined for generated mutants following bioleaching experiments with synthetic monazite and compared to the wild-type (WT) strain. *p*-value is displayed for both sets of comparisons denoting statistical significance after unpaired *t*-tests performed against WT. Blue squares indicate the mean extraction for each strain, the center line denotes the median, boxes show the upper and lower quartiles, and whiskers extend to the range of data points within 1.5 times the interquartile range.

in bioleaching, though further investigation would be necessary to confirm this.

The LysR substrate binding domain binds specific ligands for signal recognition, and as a result, triggers the activity of transcriptional regulators[62]. Its disruption may influence gene repression or activation, altering the metabolic flux in a manner favorable for bioleaching. The regulatory protein YafY presents HTH (helix-turn-helix) and WYL (tryptophan, W; tyrosine, Y; and leucine, L) domains, which are known for their role in gene expression in response to DNA damage[63]. Disruption of the hypothetical protein GO_102 produced the second-largest increase in Nd-bioleaching (Fig. 3). *blastp* analysis[64] revealed 100% sequence alignment between GO_102 and an HTH-domain containing protein, suggesting it might also be involved in gene expression. These disruptions may lead to significant changes in gene expression levels, which could explain the increase in extraction.

Both δ*GO_102* and δ*GO_1109* disruption mutants decreased biolixiviant pH but were not identified by our earlier acid production screen. The pH changes caused by these mutants are modest compared with prominent mutants from our earlier acid production screen (which decreased pH by 0.1 to 0.2 units)[16]. We suspect that these pH changes were too small to be

detected by our earlier screen. This leads us to presume that these mutants may be simultaneously altering acid and non-acid mechanisms of bioleaching.

We speculate that disruption of the hypothetical protein GO_2946 might enhance bioleaching by increasing the permeability of the outer membrane of *G. oxydans*. *blastp* analysis[64] showed homology of GO_2946 to a glycosyltransferase family 2 (GT2) protein, whose function involves the transfer of sugar moieties among intermediates during the biosynthesis of polysaccharides[65]. In a previous study, a GT2 protein was found to repress oxidative fermentation in *Gluconacetobacter intermedius*; and when disrupted, final yields of gluconic acid and acetic acid increased compared to the parental strain[65]. Changes in the polysaccharide composition of the cell surface might increase the permeability of the membrane, facilitating the diffusion of substrate, therefore enhancing transport of the biolixiviant out of the cell[65].

The disruption of a TonB-dependent receptor gene (*GO_19*) increased bioleaching. This type of system is often associated with the uptake of iron bound to siderophores[66]. Under iron starvation conditions, bacterial cells tend to upregulate secretory mechanisms in an attempt to manage iron deficiency[67,68]. Disruption of this gene might alter iron sensing and transport, prompting the cell to increase biolixiviant production.

Disruption of genes involved in nucleotide metabolism increased bioleaching (*GO_1598*, *GO_1113*, and *GO_2555*). The largest increase in bioleaching was produced by δ*GO_1598*. *GO_1598* codes for the orotate phosphoribosyltransferase enzyme PyrE which catalyzes the production of orotidine monophosphate (OMP), using phosphoribosyl diphosphate (PRPP) and orotate[69]. One way that the disruption of *GO_1598* could increase bioleaching is by increasing availability of orotate, which is known to chelate metals[69], and in particular lanthanides[70]. *GO_1113* codes for XdhC, an accessory protein involved in purine metabolism that binds to Molybdenum Cofactor (MoCo) for maturation of xanthine dehydrogenase[71]. We speculate that its disruption could create an accumulation of MoCo, and accelerate other enzymatic reactions used in the production of the biolixiviant. *GO_2555* codes a hypothetical protein that demonstrated partial homology[64] (E-value = 1×10^{-125}) to the L-dopachrome tautomerase yellow-f2 protein (EC 5.3.2.3) involved in tyrosine metabolism, which interacts with quinone and flavonoids to produce melanin[72–74]. The enhanced bioleaching observed from this disruption may be attributed to the accumulation of intermediates, which can be utilized in other metabolic pathways associated with bioleaching.

Our results propose that the choice of bioleaching substrate plays a crucial role in determining the extent to which genetic modifications lead to measurable differences in bioleaching performance. This effect likely arises because of the biochemical activity of *G. oxydans* in the presence of different minerals, altering the metabolic pathways at play during direct bioleaching. For example, in our previous work on retorted phosphor powder, the largest single-target genetically induced improvement—an 18% increase—was achieved by disrupting the *pstC* gene[16]. Similarly, an engineered knockout/overexpression strain of *G. oxydans* (with a *pstS* deletion and *mgdh* overexpression via the P112 promoter) improved bioleaching from the mineral allanite by up to 73%[15]. However, in this study using monazite, single gene disruptions improved bioleaching by as much as 111%, while the same engineered knockout/overexpression strain resulted in a striking 1186% increase over proxy wild-type. These differences suggest that the interplay between microbial activity and metal solubilization is influenced by subtle substrate-associated factors that have yet to be fully elucidated.

The construction of an engineered strain overexpressing *GO_1096* confirmed its potential as a promising target for enhancing REE extraction (Fig. 5), underscoring its involvement in the bioleaching mechanism. Although overexpression of *GO_1096* resulted in a 7.6-fold increase in gene expression, the corresponding improvements in REE extraction were not strictly proportional, suggesting that *GO_1096* likely operates within a broader genetic framework, potentially requiring the coordinated expression of additional genes to achieve optimal bioleaching effects. Moreover, the stark difference in performance between δ*GO_1096* and Δ*GO_1096*

strains indicates that the complete removal of *GO_1096* does not drastically impair the bioleaching process, hinting at possible compensatory or redundant pathways that mitigate its loss, a phenomenon previously reported in other studies[75,76]. In addition, the partial disruption in δ*GO_1096* may inadvertently affect the nearby regulatory elements or neighboring genes, leading to a more pronounced impact on bioleaching. Further investigation would be necessary to fully elucidate the precise role of *GO_1096* during bioleaching. Nevertheless, the observed benefits from its overexpression offer a promising outlook, indicating that targets identified in this study hold potential for meaningful improvements in bioleaching.

It remains unclear whether modification of other genes discussed in this article could lead to transformative advancements in bioleaching by *G. oxydans*. It is worth noting that when we first observed the effects generated by transposon disruption mutants, they were very modest compared to the improvements achieved by subsequently engineering the same target genes. For example, disruption of *pstS* only increased bioleaching from retorted phosphor powder by 4.3%[16], whereas clean deletion of *pstS* improved bioleaching from allanite by 30%[15]. Remarkably, combination of this knockout with upregulation of *mgdh* increased bioleaching from allanite by 73%[15]. This suggests—though further testing is necessary—that multiple modifications inspired by the results presented here could have substantial impacts on bioleaching performance from certain substrates.

Conclusion
Our work pivots away from the well-characterized acidolysis mechanism to examine contributions to bioleaching via alternative routes. Our findings introduce additional genes that influence bioleaching yet remained undetected in acidification screens (Figs. 2 and 3). Most genes that we identified do not significantly affect biolixiviant pH (Fig. 4).

These results, along with earlier observations by Reed et al.[21], strongly suggest that the bioleaching mechanism of *G. oxydans* is not purely acid-based. Our data suggests that disrupting genes involved in nucleotide synthesis, transcriptional regulation, DNA repair, nutrient uptake, and oxidative stress response could significantly impact bioleaching. But there is no clear evidence in this list that suggests a single gene coding for a redox molecule (e.g., a flavin) or chelator (e.g., a siderophore) amplifies the effectiveness of bioleaching.

The gene disruptions we have identified appear to be involved in regulatory functions. This suggests that if there are genes involved in complexolysis or redoxolysis within the *G. oxydans* genome, they could be multiply redundant, and that knocking out a single gene contributes only marginally to changes in bioleaching. Alternatively, these genes may possess some degree of essentiality, rendering their identification challenging. This highlights the need for broader and higher-sensitivity screening approaches that can capture a more diverse array of bioleaching-related genetic activities, potentially leading to enhanced methods for harnessing and optimizing the bioleaching mechanism.

Further research remains necessary to fully elucidate the complexities of *G. oxydans*' biolixiviant and its interaction with REEs. The integration of advanced analytical techniques may be required to precisely characterize the metabolic impact of the strains examined in this study and to identify the key components involved in REE-bioleaching.

Materials and methods
Curation of the quality-controlled whole-genome knockout collection
The QC collection was built by removing redundancy from an earlier condensed collection (CC) of *G. oxydans* transposon mutants and supplementing with additional mutants from a saturating-coverage progenitor collection (PC) from the same work[16]. The progenitor collection of transposon mutants was cataloged using the Knockout Sudoku probabilistic inference combinatorial pooling method[52,77].

The best-choice disruption mutant for each gene in the QC collection was selected by considering the location of the transposon disruption in the gene, and the reliability of the location assignment of the mutant. We

followed the generally accepted consensus that the best location for a transposon to disrupt gene function is between 50 bp from the start of the coding region and the middle of the gene (a fractional distance of ≤ 0.5 into the gene). Furthermore, we preferred to select mutants whose location was directly inferred by the Knockout Sudoku algorithm (also known as unambiguous location inference[52,77]), rather than relying upon probabilistic location inference (also known as ambiguous location inference[52,77]). If given the choice between a mutant with non-ideal locations and unambiguous location inference, and a mutant in the same gene with ideal location and ambiguous location inference, we chose the former. Mutant genomic location statistics are shown in Table 1. A catalog of the QC collection is included in Supplementary Data 1.

Mutants were transferred from the earlier collections by fluid transfer with a colony picking robot (CP7200, Norgren Systems, Ronceverte, West Virginia, USA) into fresh 96-well polypropylene storage plates containing yeast peptone mannitol (YPM) media (5 g L⁻¹ yeast extract (C7341, Hardy Diagnostics, Santa Maria, California, USA); 3 g L⁻¹ peptone (211677, BD, Franklin Lakes, New Jersey, USA); 25 g L⁻¹ mannitol (BDH9248, VWR Chemicals, Radnor, Pennsylvania, USA)) and 100 µg mL⁻¹ kanamycin. Plates were incubated at 30 °C and 800 rpm in a Multitron shaker (Infors Inc., Laurel, Maryland, USA) for 3 nights to achieve saturation. Following incubation, stocks were prepared by adding glycerol (G5516, Sigma-Aldrich, St. Louis, Missouri, USA) to 20% (v/v) to each well for long-term storage at −80 °C.

Genome-scale REE-bioleaching screen
REE concentrations were measured using the REE-Chelating Dye Arsenazo-III (As-III; 110107, Sigma-Aldrich, St. Louis, Missouri, USA). The As-III solution was prepared following the method described by Hogendoorn et al.[40].

The high-throughput screen consisted of a preliminary survey carried out in duplicate followed by a validation screen performed in triplicate. It spanned several weeks and was partitioned into batches of 10–15 plates. Plates containing disruption mutants to be analyzed were replicated from the QC collection using a 96-pin cryo-replicator press (CR1100, EnzyScreen, Heemstede, Netherlands) into 96-well polypropylene round-bottom plates filled with 150 µL YPM supplemented with 100 µg mL⁻¹ kanamycin.

Replicated plates were incubated for two nights at 30 °C, 80% humidity, and 800 rpm in a Multitron shaker. Then, cultures were back-diluted either in duplicate or triplicate, by inoculating 5 µL of bacterial culture in 120 µL of the same medium using the PlateMaster pipetting system (F110761, Gilson Inc., Middleton, Wisconsin, USA). After two nights of incubation, the optical density was measured using a plate reader (18531, Biotek, Charlotte, Vermont, USA), and the biolixiviant production was set up by measuring the remaining volume in each well and adding glucose (0188, VWR Chemicals, Radnor, Pennsylvania, USA) to 20% w/v. Plates were incubated for 24 h at 30 °C, 80% humidity, and 800 rpm. For all the aforementioned steps, 96-well plates were covered with a breathable rayon film (60941-086, VWR Chemicals, Radnor, Pennsylvania, USA).

For bioleaching, 150 µL of biolixiviant was transferred from each well into plates containing synthetic monazite powder. Plates were sealed with an adhesive polypropylene sealing Film (PCR-TS, Axygen Scientific, Union City, CA) and incubated for 24 h at 30 °C and 800 rpm. Final plates containing the leachate were centrifuged at 3214 × *g* for 12 min to obtain the supernatant to be used for analysis.

For the preliminary survey, bioleaching was performed in presence of synthetic monazite mineral Mon1 (Supplementary Data 3A) at 0.33% pulp density to facilitate an initial identification of disruption strains with differential bioleaching capabilities. For the screen with Mon2 (Supplementary Data 3C), the pulp density was 1%. After centrifugation, a 1:10 dilution of the supernatant from each well was transferred to polystyrene flat-bottom 96-well plates filled with 100 µL of 60 µM As-III Solution. For validation with Mon2, 100 µL of the supernatant was used instead. Analysis plates were shaken for 1 min, then the absorbance at 650 nm was measured with the plate reader.

REE-bioleaching screen analysis

Several factors were considered to confirm the quality of the data collected, namely cross-contamination of wells, systematic differences among wells caused by their position in the plate, and additional errors generated during manipulation.

To address these challenges, the raw data collected through our preliminary high-throughput survey with Mon1 was analyzed with a correcting software[78] to detect and remove systematic errors. This software allowed us to normalize our data based on Z-score transformation within plates[79]. To avoid false positives caused by mutants with large growth defects, wells with growth $OD_{600} < 0.2$ were excluded to avoid the potential offsets during the normalization process.

An initial hit identification was carried out by comparing the normalized absorbance values of the disruption mutants to the mean of the plate in which they were analyzed. Using a conservative threshold, disruption mutants with absorbance values deviating by more than 1.5 standard deviations from the plate mean were selected for further screening.

For our screen with Mon2, wells containing the selected disruption mutants were used to inoculate new 96-well plates filled with medium supplemented with antibiotic. To ensure reliable data collection, we arrayed the mutants in a checkerboard pattern, included each mutant in triplicate, avoided perimeter wells to reduce medium evaporation, and included a proxy wild-type strain within each plate.

Raw absorbance data was used for statistical analysis, which included pairwise comparisons conducted utilizing the emmeans package in R while applying a false discovery rate (FDR) correction for p-value adjustment for multiple comparisons[80]. Disruption mutants that demonstrated significant differences in REE-extraction were considered promising.

Gene ontology enrichment analysis

A gene ontology (GO) enrichment analysis was carried out as described by Schmitz et al.[16]. Enrichment was performed with the BioConductor topGO package[45,81], employing the TopGO Fisher test with the default weight algorithm, applying a significance threshold of 0.05.

Direct REE-bioleaching measurements

Selected disruption mutants that included six significant hits identified through the REE-bioleaching screen and other six additional disruption mutants were used for further validation through bench-scale bioleaching experiments[82] with Mon2. Additional disruption mutants were picked based on the features disrupted that represented a trait of interest, these included specific enzymes or disruptions with interesting behavior throughout the screen.

A total of 12 disruption mutant strains were plated on YPM and kanamycin agar (05039, VWR Chemicals, Radnor, PA) for colony isolation. Three biological replicates for each disruption mutant were used to inoculate 3 mL cultures, as well as for wild-type controls in addition to no-bacteria control. After incubation for two nights at 30 °C and 200 rpm in a shaking incubator (29314, Infors Inc., Laurel, MD), cultures were normalized to OD_{590} 0.01 in 50 mL flasks with a final volume of 5 mL and grown for another two nights. Following incubation, the cultures were diluted 1:1 with glucose 40% (w/v) to reach a final concentration of 20%. Flasks were incubated at 30 °C and 200 rpm for 48 h to allow biolixiviant production.

Bioleaching experiments were set up to digest Mon2 at 1% pulp density, for 24 h at 30 °C and 200 rpm. Once obtained, the leachate was filtered through a 0.45 μm AcroPrep Advance 96-well filter plate (8029, Pall Corporation, Show Low, AZ, USA) by centrifugation at $1500 \times g$ for 5 min.

Each sample underwent a 20-fold dilution using 2% trace metal grade nitric acid (JT9368, J.T. Baker, Radnor, Pennsylvania, USA). Neodymium concentration in each sample was measured using an Agilent 7800 ICP-MS. Calibration and verification utilized a REE mix standard (67349, Sigma-Aldrich, St. Louis, Missouri, USA) and a rhodium internal standard (04736, Sigma-Aldrich, $m/Z = 103$). Rigorous quality checks included intermittent assessment of standards, blanks, and replicate samples[83]. Data interpretation was carried out using MassHunter software, version 4.5.

A proxy wild-type strain (pWT) was selected for comparison to account for changes in the wild-type background introduced by the presence of the antibiotic cassette in the genome. The selected pWT contains a transposon insertion in an intergenic region (at base pair 1,262,471; between genes *GO_2147* and *GO_2148*) and does not demonstrate any notable phenotypic changes. This strain can be located in plate 130, well A2 in the progenitor collection.

For each disruption mutant, bioleaching measurements ($n = 3$) were evaluated against those of the wild-type and proxy wild-type strains ($n = 3$). This was done performing pairwise comparisons with Bonferroni correction using the emmeans package in R. The total REE extracted was deemed significantly different if $p < 0.05/N$ ($N = 12$).

Genetic engineering

The gene *GO_1096* was selected as the target for genetic engineering experiments to validate screen results. Engineered strains generated in this study included the clean deletion of *GO_1096* and the overexpression of *GO_1096* via the P_{112} promoter. Genetic modifications were introduced using the *codA/codB*-based counterselection system[84] for allelic exchange. The suicide vector pKOS6b was linearized with XbaI (FD0684, Thermo Fisher Scientific, Waltham, MA) and used as the backbone for cloning.

To generate a deletion of *GO_1096*, a thousand base pair regions immediately upstream and downstream of the target locus were amplified and assembled into the linearized pKOS6b using the HiFi DNA Assembly Kit (E5520, New England Biolabs, Ipswich, MA). For transcriptional upregulation of *GO_1096*, the promoter P_{112}, flanked by a thousand base pairs upstream and downstream of the *GO_1096* start site, was cloned into pKOS6b.

Plasmids were transformed into *G. oxydans* by electroporation, following the protocol described by Mostafa et al.[85]. Briefly, *G. oxydans* cells were harvested at an optical density of 0.8 and washed three times with 1 mM HEPES buffer. The final pellet was resuspended in 250 μL of HEPES and glycerol to 12%, flash-frozen in liquid nitrogen, and stored at −80 °C. For transformation, thawed cells were electroporated with 250 ng of plasmid DNA at 2 kV for 3 ms, using the Bio-Rad MicroPulser (1652100, Bio-Rad, Hercules, CA). Cells were then recovered in 800 μL of EP medium (80 g L^{-1} mannitol, 15 g L^{-1} yeast extract, 2.5 g L^{-1} MgSO$_4$·7H$_2$O, 1.5 g L^{-1} CaCl$_2$, and 0.5 g L^{-1} glycerol) and incubated overnight. Following recovery, cells were plated on EP agar supplemented with 100 μg mL^{-1} kanamycin to select for integrants. Colonies were subsequently patched onto YPM agar containing 10 μg mL^{-1} 5-fluorocytosine (5-FC) (F0321, VWR Chemicals, Radnor, PA) for counterselection. Colonies emerging on 5-FC plates were screened using colony PCR. Successful mutants were confirmed by sequencing to verify the intended modification. Strains and plasmids used in this work are listed in Table S2, and oligonucleotides in Table S3.

Gene expression analysis

To assess the effectiveness of the promoter in the overexpressed strain, changes in expression levels were determined by real-time quantitative polymerase chain reaction (RT-qPCR) with QuanStudio7 Pro (Thermo Fisher Scientific, Waltham, MA). Extraction of microbial RNA was achieved using the RNeasy mini kit (74524, Qiagen, Hilden, Germany), following the manufacturer's protocols for enzymatic lysis and proteinase K digestion of bacteria, and purification of total RNA from bacterial lysate. cDNA synthesis and amplification were conducted using the Luna Universal One-Step RT-qPCR kit (E3005, New England Biolabs, Ipswich, MA). The *gap* gene was used as the internal reference (housekeeping gene) for normalization. All experiments were performed in triplicate with biological replicates.

Limitations of the study

During high-throughput screening, growth hindrance due to strain disruption poses considerable challenges. For example, despite the *pstS* gene disruption being flagged as a key player in REE-bioleaching during preliminary testing, its pronounced effect on microbial growth required its exclusion from final analyses because it did not meet the established growth threshold for inclusion. Future studies could address these growth-related

issues by incorporating an upregulation collection into the screening process. This approach would not only enhance the insights gained from knockout collections but also allow for the potential identification of essential genes as significant contributors to bioleaching.

Other limitations involve the choice of the colorimetric reporter As-III. This dye was selected based on extensive evidence of its high binding affinity to REE; however, while the formation constant of this chelator is relatively high[86,87], there is potential for underreporting of hits containing stronger chelators that could interfere with dye-REE complex formation. As a result, the associated gene disruptions may not have been identified due to competition in REE binding during screening. Additional screening strategies would be necessary to account for such competitive interactions.

Furthermore, confirmation of gene involvement of hits identified in this study will require further experiments, including gene deletion and complementation, to fully evaluate gene function and interaction.

While our study adds to the growing body of work on microbial metal recovery, the application of engineered microbes in bioleaching is still emerging. Successes have been noted with engineered strains in controlled settings such as stirred-tank reactors. Nonetheless, advancing this technology will require careful consideration of containment strategies and regulatory adjustments to appropriately mitigate potential risks.

Statistics and reproducibility
In our genome-scale screen, statistical robustness was ensured through multiple replicates and a rigorous validation approach. Our screen included a preliminary survey carried out in duplicate, followed by a validation screen performed in triplicate. This multistep approach allowed for the establishment of robustness in our findings. To control for potential biases, we considered factors such as cross-contamination of wells, position-related systematic noise, and errors during manipulation.

The data from our preliminary survey with Mon1 was corrected using specialized software to remove systematic errors[78], and Z-score transformation was applied within plates for normalization. Wells that showed growth OD_{600} below 0.2 were excluded to avoid potential offsets during this normalization process. Disruption mutants exhibiting changes of 1.5 standard deviations from the plate mean were selected for further screening.

In the subsequent validation screen with Mon2, disruption mutants were subjected to a more stringent validation process. This included a balanced distribution of mutants across the plates, triplicate data collection, and within-plate comparison strains. Statistical significance for the REE-extraction capabilities of each mutant was determined using pairwise comparisons with the emmeans package in R and applying a false discovery rate (FDR) correction for p-value adjustment in multiple comparisons.

Bench-scale bioleaching experiments further confirmed the reproducibility of our findings, with each mutant strain's performance benchmarked against that of the wild-type and the proxy wild-type strains. Neodymium extraction levels measured by ICP-MS were compared pairwise, with significance established at $p < 0.05$ after Bonferroni correction ($N = 12$). These stringent statistical analyses ensured that the results presented were both robust and reproducible, providing a reliable foundation for future explorations into the genetic determinants of REE-bioleaching.

Reporting summary
Further information on research design is available in the Nature Portfolio Reporting Summary linked to this article.

Data availability
Datasets generated and analyzed during this study are included with this article and are available at https://github.com/barstowlab/article-036-non-acid-bioleaching. They are also archived on Zenodo[88].

Code availability
Code used in the generation of figures and analysis of data for this article is available at https://github.com/barstowlab/article-036-non-acid-bioleaching and is also archived on Zenodo[88].

Materials availability
Material requests should be addressed to B.B. Individual strains (up to ≈10 at a time) are available at no charge for academic researchers. We are happy to supply a duplicate of the entire *G. oxydans* knockout collection to academic researchers but will require reimbursement for materials, supplies, and labor costs. Commercial researchers should contact Cornell Technology Licensing for licensing details. *E. coli* strains harboring plasmids used for genetic modification of *G. oxydans* have been deposited at Addgene under accession codes 238022 (pKOS6b-P112_GO1096) and 238023 (pKOS6b-KOGO1096).

References
1. Dent, P. C. Rare earth elements and permanent magnets (invited). *J. Appl. Phys.* **111**. https://doi.org/10.1063/1.3676616 (2012).
2. Bauer, D. et al. U.S. Department of Energy Critical Materials Strategy. Medium: ED (United States, 2010).
3. Humphries, M. Rare Earth Elements: The Global Supply Chain. Report No. https://digital.library.unt.edu/ark:/67531/metadc272008/ (2013).
4. Schubert, E. F. & Kim, J. K. Solid-state light sources getting smart. *Science* **308**, 1274–1278 (2005).
5. Peng, F. et al. Hydrogen clathrate structures in rare earth hydrides at high pressures: possible route to room-temperature superconductivity. *Phys. Rev. Lett.* **119**, 107001 (2017).
6. Ivanovskii, A. L. New high-temperature superconductors based on rare-earth and transition metal oxyarsenides and related phases: synthesis, properties and simulations. *Phys.Uspekhi* **51**, 1229 (2008).
7. Zurek, E. & Bi, T. High-temperature superconductivity in alkaline and rare earth polyhydrides at high pressure: a theoretical perspective. *J. Chem. Phys.* **150**. https://doi.org/10.1063/1.5079225 (2019).
8. International Energy Agency. The Role of Critical Minerals in Clean Energy Transitions. https://www.iea.org/reports/the-role-of-critical-minerals-in-clean-energy-transitions (2021).
9. Castro, L., Blázquez, M. L., González, F. & Muñoz, J. Biohydrometallurgy for rare earth elements recovery from industrial wastes. *Molecules* **26**. https://doi.org/10.3390/molecules26206200 (2021).
10. Bauer, D. et al. Critical Materials Strategy. (U.S. Department of Energy, 2011).
11. Lucas, J., Lucas, P., Le Mercier, T., Rollat, A. & Davenport, W. In *Rare Earths* (eds Lucas, J. et al.) 47–67 (Elsevier, 2015).
12. Rasoulnia, P., Barthen, R. & Lakaniemi, A.-M. A critical review of bioleaching of rare earth elements: The mechanisms and effect of process parameters. *Crit. Rev. Environ. Sci. Technol.* **51**, 378–427 (2021).
13. Brisson, V. L., Zhuang, W.-Q. & Alvarez-Cohen, L. Bioleaching of rare earth elements from monazite sand. *Biotechnol. Bioeng.* **113**, 339–348 (2016).
14. Thompson, V. S. et al. Techno-economic and life cycle analysis for bioleaching rare-earth elements from waste materials. *ACS Sustain. Chem. Eng.* **6**, 1602–1609 (2018).
15. Schmitz, A. M. et al. High efficiency rare earth element biomining with systems biology guided engineering of gluconobacter oxydans. *bioRxiv*, 2023.2002.2009.527855. https://doi.org/10.1101/2023.02.09.527855 (2023).
16. Schmitz, A. M. et al. Generation of a Gluconobacter oxydans knockout collection for improved extraction of rare earth elements. *Nat. Commun.* **12**, 6693 (2021).
17. Bonificio, W. D. & Clarke, D. R. Rare-earth separation using bacteria. *Environ. Sci. Technol. Lett.* **3**, 180–184 (2016).
18. Medin, S. et al. Genomic characterization of rare earth binding by Shewanella oneidensis. *Sci. Rep.* **13**, 15975 (2023).

19. Mattocks, J. A. & Cotruvo, J. A. Biological, biomolecular, and bio-inspired strategies for detection, extraction, and separations of lanthanides and actinides. *Chem. Soc. Rev.* **49**, 8315–8334 (2020).

20. Skovran, E. & Martinez-Gomez, N. C. Just add lanthanides. *Science* **348**, 862–863 (2015).

21. Reed, D. W., Fujita, Y., Daubaras, D. L., Jiao, Y. & Thompson, V. S. Bioleaching of rare earth elements from waste phosphors and cracking catalysts. *Hydrometallurgy* **166**, 34–40 (2016).

22. Gumulya, Y. et al. In a quest for engineering acidophiles for biomining applications: challenges and opportunities. *Genes* **9**, 116 (2018).

23. Vera, M., Schippers, A., Hedrich, S. & Sand, W. Progress in bioleaching: fundamentals and mechanisms of microbial metal sulfide oxidation—part A. *Appl. Microbiol. Biotechnol.* **106**, 6933–6952 (2022).

24. Naseri, T., Beiki, V., Mousavi, S. M. & Farnaud, S. A comprehensive review of bioleaching optimization by statistical approaches: recycling mechanisms, factors affecting, challenges, and sustainability. *RSC Adv.* **13**, 23570–23589 (2023).

25. Shen, L., Zhou, H., Qiu, G. & Zhao, H. A review of bioleaching combined with low-cost fermentation and metabolic engineering technology to leach rare earth elements. *J. Environ. Chem. Eng.* **12**, 112117 (2024).

26. De Muynck, C. et al. The genus gluconobacter oxydans: comprehensive overview of biochemistry and biotechnological applications. *Crit. Rev. Biotechnol.* **27**, 147–171 (2007).

27. Kazunobu Matsushita, H. T., Naoto Tonouchi, Akiko Okamoto-Kainuma. *Acetic Acid Bacteria*. 350 (Springer, 2016).

28. Macauley, S., McNeil, B. & Harvey, L. M. The genus gluconobacter and its applications in biotechnology. *Crit. Rev. Biotechnol.* **21**, 1–25 (2001).

29. Ripoll, M., Lerma-Escalera, J. A., Morones-Ramírez, J. R., Rios-Solis, L. & Betancor, L. New perspectives into gluconobacter-catalysed biotransformations. *Biotechnol. Adv.* **65**, 108127 (2023).

30. Antonick, P. J. et al. Bio- and mineral acid leaching of rare earth elements from synthetic phosphogypsum. *J. Chem. Thermodyn.* **132**, 491–496 (2019).

31. Jin, H. et al. Sustainable bioleaching of rare earth elements from industrial waste materials using agricultural wastes. *ACS Sustain. Chem. Eng.* **7**, 15311–15319 (2019).

32. Owusu-Fordjour, E. Y. & Yang, X. Bioleaching of rare earth elements challenges and opportunities: a critical review. *J. Environ. Chem. Eng.* **11**, 110413 (2023).

33. Vo, P. H. N. et al. Biomining for sustainable recovery of rare earth elements from mining waste: a comprehensive review. *Sci. Total Environ.* **908**, 168210 (2024).

34. Bosecker, K. Bioleaching: metal solubilization by microorganisms. *FEMS Microbiol. Rev.* **20**, 591–604 (1997).

35. Abhilash, Hedrich, S. & Schippers, A. Distribution of scandium in red mud and extraction using gluconobacter oxydans. *Hydrometallurgy* **202**, 105621 (2021).

36. Abhilash et al. Extraction of REEs from blast furnace slag by gluconobacter oxydans. *Minerals* **12**, 701 (2022).

37. Rasoulnia, P., Barthen, R., Puhakka, J. A. & Lakaniemi, A.-M. Leaching of rare earth elements and base metals from spent NiMH batteries using gluconate and its potential bio-oxidation products. *J. Hazard. Mater.* **414**, 125564 (2021).

38. Banerjee, I., Burrell, B., Reed, C., West, A. C. & Banta, S. Metals and minerals as a biotechnology feedstock: engineering biomining microbiology for bioenergy applications. *Curr. Opin. Biotechnol.* **45**, 144–155 (2017).

39. Corbett, M. K., Eksteen, J. J., Niu, X.-Z., Croue, J.-P. & Watkin, E. L. J. Interactions of phosphate solubilising microorganisms with natural rare-earth phosphate minerals: a study utilizing Western Australian monazite. *Bioprocess Biosyst. Eng.* **40**, 929–942 (2017).

40. Hogendoorn, C. et al. Facile Arsenazo III-based assay for monitoring rare earth element depletion from cultivation media for methanotrophic and methylotrophic bacteria. *Appl. Environ. Microbiol.* **84**, e02887–02817 (2018).

41. Rohwer, H., Collier, N. & Hosten, E. Spectrophotometric study of Arsenazo III and its interactions with lanthanides. *Anal. Chim. Acta* **314**, 219–223 (1995).

42. Balta, J., Holycross, M. E., Barstow, B. & Gazel, E. Co-generation of NaREE(MoO$_4$)$_2$ and REEPO$_4$ in multiple habits by solid-flux crystal growth. *SSRN.* https://doi.org/10.2139/ssrn.4833307 (2024).

43. Brierley, C. L. Microbiological mining. *Sci. Am.* **247**, 44–53 (1982).

44. Charkin, D. O. et al. Structural, thermal, and IR studies of β-[Nd2O2] (CrO4), an unexpected analog of a slag phase [Ba2F2](S6+O3S2−). *Z. für Kristallographie—Crystalline Mater.* **234**, 1–8 (2019).

45. Alexa, A. & Rahnenfuhrer, J. topGO: Enrichment Analysis for Gene Ontology. R package version 2.59.0 (2024).

46. Capdevila, D. A., Edmonds, K. A. & Giedroc, D. P. Metallochaperones and metalloregulation in bacteria. *Essays Biochem.* **61**, 177–200 (2017).

47. Chunqiang Zhang, F. Z., Zhou, P. & Zhang, C. Functional role of metalloproteins in genome stability. *Front. Biol.* **11**, 119–131 (2016).

48. Nakayama, H. In *Handbook of Metal Biotechnology* (ed Mitsuo Yamashita Michihiko Ike, Satoshi Soda) Ch. 17, 32 (Jenny Stanford Publishing, 2012).

49. Urbina, J. et al. A new approach to biomining: bioengineering surfaces for metal recovery from aqueous solutions. *Sci. Rep.* **9**, 16422 (2019).

50. Carvajal-Garcia, J., Samadpour, A. N., Hernandez Viera, A. J. & Merrikh, H. Oxidative stress drives mutagenesis through transcription-coupled repair in bacteria. *Proc. Natl Acad. Sci.* **120**, e2300761120 (2023).

51. Fan, Y. et al. Protein mistranslation protects bacteria against oxidative stress. *Nucleic Acids Res.* **43**, 1740–1748 (2015).

52. Baym, M., Shaket, L., Anzai, I. A., Adesina, O. & Barstow, B. Rapid construction of a whole-genome transposon insertion collection for Shewanella oneidensis by Knockout Sudoku. *Nat. Commun.* **7**, 13270 (2016).

53. Giaever, G. & Nislow, C. The yeast deletion collection: a decade of functional genomics. *Genetics* **197**, 451–465 (2014).

54. Gallagher, L. A. et al. Sequence-defined transposon mutant library of Burkholderia thailandensis. *mBio* **4**, e00604–e00613 (2013).

55. Sousa, M. et al. Genome-wide identification of genes involved in the positive and negative regulation of acetic acid-induced programmed cell death in Saccharomyces cerevisiae. *BMC Genomics* **14**, 838 (2013).

56. Landová, B. & Šilhán, J. Conformational changes of DNA repair glycosylase MutM triggered by DNA binding. *FEBS Lett.* **594**, 3032–3044 (2020).

57. Pittman, M. S., Robinson, H. C. & Poole, R. K. A bacterial glutathione transporter (Escherichia coli CydDC) exports reductant to the periplasm*. *J. Biol. Chem.* **280**, 32254–32261 (2005).

58. Kumar, V. et al. Structure of BipA in GTP form bound to the ratcheted ribosome. *Proc. Natl Acad. Sci.* **112**, 10944–10949 (2015).

59. Jha, V., Dafale, N. A. & Purohit, H. J. Regulatory rewiring through global gene regulations by PhoB and alarmone (p)ppGpp under various stress conditions. *Microbiol. Res.* **227**, 126309 (2019).

60. Yamada, M., Makino, K., Shinagawa, H. & Nakata, A. Regulation of the phosphate regulon of Escherichia colt properties of phoR deletion mutants and subcellular localization of PhoR protein. *Mol. Gen. Genet. MGG* **220**, 366–372 (1990).

61. Lubin, E. A., Henry, J. T., Fiebig, A., Crosson, S. & Laub, M. T. Identification of the PhoB regulon and role of PhoU in the phosphate starvation response of Caulobacter crescentus. *J. Bacteriol.* **198**, 187–200 (2016).

62. Matilla, M. A., Velando, F., Martín-Mora, D., Monteagudo-Cascales, E. & Krell, T. A catalogue of signal molecules that interact with sensor kinases, chemoreceptors and transcriptional regulators. *FEMS Microbiol. Rev.* **46**. https://doi.org/10.1093/femsre/fuab043 (2021).

63. Keller, L. M. L., Flattich, K. & Weber-Ban, E. Novel WYL domain-containing transcriptional activator acts in response to genotoxic stress in rapidly growing mycobacteria. *Commun. Biol.* **6**, 1222 (2023).

64. Camacho, C. et al. BLAST+: architecture and applications. *BMC Bioinforma.* **10**, 421 (2009).

65. Iida, A., Ohnishi, Y. & Horinouchi, S. Identification and characterization of target genes of the GinI/GinR quorum-sensing system in Gluconacetobacter intermedius. *Microbiology* **155**, 3021–3032 (2009).

66. Delepelaire, P. Bacterial ABC transporters of iron containing compounds. *Res. Microbiol.* **170**, 345–357 (2019).

67. Folsom, J. P., Parker, A. E. & Carlson, R. P. Physiological and proteomic analysis of Escherichia coli iron-limited chemostat growth. *J. Bacteriol.* **196**, 2748–2761 (2014).

68. Sasnow, S. S., Wei, H. & Aristilde, L. Bypasses in intracellular glucose metabolism in iron-limited Pseudomonas putida. *MicrobiologyOpen* **5**, 3–20 (2016).

69. Silva, R., Aguiar, T. Q. & Domingues, L. Orotic acid production from crude glycerol by engineered Ashbya gossypii. *Bioresour. Technol. Rep.* **17**, 100992 (2022).

70. Kostova, I., Mojžiš, J. & Chiş, V. Theoretical and experimental vibrational characterization of biologically active Nd(III) complex. *Molecules* **26**, 2726 (2021).

71. Neumann, M., Schulte, M., Jünemann, N., Stöcklein, W. & Leimkühler, S. Rhodobacter capsulatus XdhC is involved in molybdenum cofactor binding and insertion into xanthine dehydrogenase*. *J. Biol. Chem.* **281**, 15701–15708 (2006).

72. Choi, K.-Y. Bioprocess of microbial melanin production and isolation. *Front. Bioeng. Biotechnol.* **9**. https://doi.org/10.3389/fbioe.2021.765110 (2021).

73. El-Naggar, N. E.-A. & Saber, W. I. A. Natural melanin: current trends, and future approaches, with especial reference to microbial source. *Polymers* **14**, 1339 (2022).

74. Solano, F. On the metal cofactor in the tyrosinase family. *Int. J. Mol. Sci.* **19**, 633 (2018).

75. Szamecz, B. et al. The genomic landscape of compensatory evolution. *PLOS Biol.* **12**, e1001935 (2014).

76. Wang, X. et al. Deletion of AS87_03730 gene changed the bacterial virulence and gene expression of Riemerella anatipestifer. *Sci. Rep.* **6**, 22438 (2016).

77. Anzai, I. A., Shaket, L., Adesina, O., Baym, M. & Barstow, B. Rapid curation of gene disruption collections using Knockout Sudoku. *Nat. Protoc.* **12**, 2110–2137 (2017).

78. Makarenkov, V. et al. HTS-Corrector: software for the statistical analysis and correction of experimental high-throughput screening data. *Bioinformatics* **22**, 1408–1409 (2006).

79. Kevorkov, D. & Makarenkov, V. Statistical analysis of systematic errors in high-throughput screening. *J. Biomol. Screen.* **10**, 557–567 (2005).

80. Benjamini, Y. & Hochberg, Y. Controlling the false discovery rate: a practical and powerful approach to multiple testing. *J. R. Stat. Soc. Ser. B* **57**, 289–300 (1995).

81. topGO: Enrichment Analysis for Gene Ontology. R package version 2.52.0. (2023).

82. Silberbach, M., Maier, B., Zimmermann, M. & Büchs, J. Glucose oxidation by Gluconobacter oxydans: characterization in shaking-flasks, scale-up and optimization of the pH profile. *Appl. Microbiol. Biotechnol.* **62**, 92–98 (2003).

83. Al-Hakkani, M. F. Guideline of inductively coupled plasma mass spectrometry "ICP–MS": fundamentals, practices, determination of the limits, quality control, and method validation parameters. *SN Appl. Sci.* **1**, 791 (2019).

84. Kostner, D., Peters, B., Mientus, M., Liebl, W. & Ehrenreich, A. Importance of codB for new codA-based markerless gene deletion in Gluconobacter strains. *Appl. Microbiol. Biotechnol.* **97**, 8341–8349 (2013).

85. Mostafa, H. E., Heller, K. J. & Geis, A. Cloning of *Escherichia coli* lacZ and lacY Genes and Their Expression in Gluconobacter oxydans and Acetobacter liquefaciens. *Appl. Environ. Microbiol.* **68**, 2619–2623 (2002).

86. Zhang, Z. et al. Complexation of gluconic acid with Nd(III) in acidic solutions: A thermodynamic study. *J. Alloy. Compd.* **444-445**, 470–476 (2007).

87. Kaczmarek, M., Meinrath, G., Lis, S. & Kufelnicki, A. The interaction of Arsenazo III with Nd(III)—a chemometric and metrological analysis. *J. Solut. Chem.* **37**, 933–946 (2008).

88. Marecos, S. barstowlab/article-036-non-acid-bioleaching: Article 36 Release 1.0 for Communications Biology Submission. https://doi.org/10.5281/zenodo.15132509 (2025).

Acknowledgements

Author contributions

Conceptualization, S. Marecos and B.B.; Methodology, S. Marecos and B.B.; Investigation, S. Marecos, B.P., S.A.M., A.S., and M.A.; Writing—Original draft, S. Marecos and B.B.; Writing—Review and editing, S. Marecos, B.B., J.B.B., M.W., E.G., S.A.M., and A.S.; Funding acquisition, S. Marecos, S.A.M., A.S., M.W., M.H., E.G., and B.B.; Resources, M.C.R., E.G., J.B.B., and B.B.; Supervision, M.W., M.H., E.G., M.C.R., and B.B.; Data curation, S. Marecos and B.B.; Visualization, S. Marecos and B.B.; Formal analysis, S. Marecos.

Competing interests

The authors declare the following competing interests: S. Marecos, B.P., S.A.M., A.S., and B.B. are pursuing patent protection for engineered organisms using knowledge gathered in this work (US provisional application 63/653,203). S.A.M. and A.S. are co-founders of, and B.B. is a contributor, and uncompensated advisor to, REEgen, Inc., which is developing genetically engineered microbes for REE bio-mining. The remaining authors declare no competing interests.

Additional information

Supplementary information The online version contains supplementary material available at https://doi.org/10.1038/s42003-025-08061-4.

Correspondence and requests for materials should be addressed to Buz Barstow.

Peer review information *Communications Biology* thanks Jon Marles-Wright, Paul Schweiger, and the other, anonymous, reviewer for their contribution to the peer review of this work. Primary Handling Editor: Tobias Goris.

Reprints and permissions information is available at http://www.nature.com/reprints

Publisher's note Springer Nature remains neutral with regard to jurisdictional claims in published maps and institutional affiliations.